International Journal of Modern Physics E
Vol. 19, Nos. 5 & 6 (2010) 965–976

DOI: 10.1142/S0218301310015412

BEAM ASYMMETRY Σ OF THE π^- PHOTOPRODUCTION OFF NEUTRON

G. MANDAGLIO[1,2], V. BELLINI[3,2], J. P. BOCQUET[4], L. CASANO[5], A. D'ANGELO[6,5], R. DI SALVO[5], A. FANTINI[6,5], D. FRANCO[6,5], G. GERVINO[7], F. GHIO[8], G. GIARDINA[1,2], B. GIROLAMI[8], A. GIUSA[3,2], A. S. IGNATOV[9], A. M. LAPIK[9], P. LEVI SANDRI[10], A. LLERES[4], F. MAMMOLITI[3,2], M. MANGANARO[1,2], D. MORICCIANI[5], A. N. MUSHKARENKOV[9], V. G. NEDOREZOV[9], C. RANDIERI[3,2], D. REBREYEND[4], N. V. RUDNEV[9], G. RUSSO[3,2], C. SCHAERF[6,5], M. L. SPERDUTO[3,2], M. C. SUTERA[2], A. TURINGE[9] and V. VEGNA[6,5]

[1] *Dipartimento di Fisica, Università di Messina, I-98166 Messina, Italy*
[2] *INFN, Sezione di Catania, I-95123 Catania, Italy*
[3] *Dipartimento di Fisica e Astronomia, Università di Catania, I-95123 Catania, Italy*
[4] *LPSC, Université Joseph Fourier, CNRS/IN2P3, Institut National Polytechnique de Grenoble, France*
[5] *INFN, Sezione di Roma "Tor Vergata", I-00133 Roma, Italy*
[6] *Dipartimento di Fisica, Università di Roma "Tor Vergata", I-00133 Roma, Italy*
[7] *Dipartimento di Fisica Sperimentale, Università di Torino, and INFN - Sezione di Torino, I-00125 Torino, Italy*
[8] *Instituto Superiore di Sanità, I-00161 Roma, and INFN - Sezione di Roma, I-00185 Roma, Italy*
[9] *Institute for Nuclear Research, RU-117312 Moscow, Russia*
[10] *INFN-Laboratori Nazionali di Frascati, I-00044 Frascati, Italy*
gmandaglio@unime.it

We present the analysis of data performed in order to identify the events of the $\gamma + n \rightarrow \pi^- + p$ reaction obtained by bombarding a liquid Deuterium target with a polarised γ beam of 0.55-1.5 GeV at the Graal-experiment. We show the effect of different kinematic and hardware constraints used to reduce the contamination coming from the concurrent reaction channels. By the simulation we estimate the contamination degree due to the other reaction channels so we can test the reliability of our method. We describe a new three-dimensional cut based on the Fermi momentum reconstruction and its effect on the suppression of the concurrent double charged pion photoproduction. We present the preliminary beam asymmetry Σ of the π^- fotoproduction off quasi-free neutron up to about $\theta_{\mathrm{c.m.},\pi^-} = 165^\circ$ together with some theoretical multipolar analysis. For a comparison we also report the data present in literature on the same reaction for E_γ =850-1740 MeV and $\theta_{\mathrm{c.m.},\pi^-} \leq 105^\circ$.

1. Introduction

Pseudoscalar meson photoproduction has proved to be a valid and complementary approach to hadronic reactions for the study of baryon resonances. The main dis-

advantage of the e.m. probe, i.e. the lower cross section values, has been overcome thanks to new technology (high intensity real and virtual photon beams, and large solid angle and/or large momentum acceptance detectors). Meson photoproduction can be described in terms of four complex CGLN[1] (or equivalently helicity) amplitudes, providing seven real independent quantities for each set of incident photon energy and meson polar angle in the center-of-mass (c.m.) system.

Polarization observables, accessible with the use of polarized photon beams and/or nucleon targets, and/or the measurement of the polarization of the recoil nucleon, play a special role in the disentanglement of the hadron resonances contributing to reaction[2−5].

To disentangle isoscalar and isovector transition amplitudes are necessary experiments on the proton and neutron, and the detection of charged and neutral pions in the final state. The four possible photoproduction reactions are linked together and to three independent amplitudes.[6,7]

Data on these reactions have been collected at Graal, with a polarized photon beam impinging on a H_2 or D_2 target and final products were detected in a large solid angle apparatus. Such investigations allowed for the first time the simultaneous extraction of the asymmetry values for the four reactions with the same experimental conditions and the same photon energy range (0.55-1.5 GeV), corresponding to the second and third nucleon resonance regions. Results for the first three reactions (π^+n,π^0p,π^0n) have already been published by the Graal collaboration,[8,9,10] providing for the pion photoproduction on the nucleon a very extensive database of high precision data.

The results of the asymmetry for the π^-p photoproduction on the quasi-free neutron advance the isospin study of the pion photoproduction on the nucleon, providing the possibility of a test on the validity of the isospin symmetry and a determination of the three isoscalar and isovector transition amplitudes.

We present the analysis of data in order to identify the events of the π^- meson photoproduction off neutron in Deuterium, in kinematic conditions where the neutron is protagonist and the proton is spectator. We present the procedure to identify the proton and charged pion in each reaction event, and the kinematic cuts used for the determination of the $\gamma n \to \pi^-$p reaction channel.

2. Experimetal Set-Up

The Graal γ-ray beam at the ESRF is produced by the backward scattering in flight of laser photons on the relativistic electrons circulating in the storage ring. This technique, first used for the Ladon beam on the Adone storage ring at Frascati,[11] produces polarized and tagged γ-ray beams with very high polarization and good energy resolution. At its maximum energy the polarization of the beam is very close to that of the laser photons (linear or circular)[12] and can be easily rotated or changed with conventional optical components changing the polarization of the laser light. It remains above 74% down to an energy 70% of the maximum energy.

With the 6.03 GeV ESRF accelerator and the 351 nm line of an Argon (Ion) Laser the maximum γ-ray energy obtainable is 1487 MeV and the spectrum is almost flat down to zero energy. The energy resolution is determined by the optics of the ESRF magnetic lattice and is 16 MeV (FWHM) over the entire spectrum.

The Graal apparatus has been described in several papers [8–10,13–16]. A cylindrical liquid Hydrogen (or Deuterium) target is located on the beam with its axis on the beam axis. The detector covers the entire solid angle and is divided into three parts. The central part, $25° < \theta \leq 155°$, is covered by two cylindrical wire chamber, a Barrel made of 32 plastic scintillators and a BGO crystal ball made of 480 crystals well suited for the detection of γ-rays of energy below 1.5 GeV. The chambers, the Barrel and the BGO are all coaxial with the beam and the target. The wire chambers detect and measure the positions and angles of the charged particles emitted by the target while the scintillating Barrel measures their specific ionization. The BGO ball detects charged and neutral particles and measures the energy deposited by them. For neutral particle it provides a measurement of their angles by its division in 480 (15×32) individual crystals: 15 in the θ direction and 32 in the ϕ direction.

At forward angles, $\theta \leq 25°$, the particles emitted from the target encounter first two plane wire chambers who measure their angles, then, at 3 meters from the center of the target, two planes of plastic scintillators, made of 28 horizontal and 28 vertical bars to measure the particles position, specific ionization and time of flight, and then a thick (Shower) wall made of a sandwich of scintillators and lead to detect charged particles, γ-rays and neutrons. The TOF resolution of these scintillators is of the order of 560 ps (FWHM). The total thickness of the plastic scintillators is 20 cm and the detection efficiency is about 20% for neutrons and 95% for γ-rays.

The energy of the γ-rays is provided by the tagging set-up which is located inside the ESRF shielding, attached to the ESRF vacuum system. The electrons which have scattered off a laser photon and produced a γ-ray have lost a significant fraction of their energy and therefore drift away from the equilibrium orbit of the stored electrons and finally hit the vacuum chamber of the storage ring. Before hitting the vacuum chamber they traverse the tagging detector, which measures their displacement from the equilibrium orbit. This displacement is a measure of the difference between their energy and that of the stored electron beam and therefore a measure of the energy of the gamma-ray produced. The tagging detector[9] consists of 10 plastic scintillators and a Solid State Microstrip Detector with 128 strips with a pitch of 300 μm. The plastic scintillators, followed by a GaAs electronics synchronized with the ring RF accelerating system, provide a timing for the entire electronics of the Graal apparatus with a resolution of 180 ps (FWHM). This allows a clear discrimination between electrons coming from two adjacent electron bunches that are separated by 2.8 ns. The Microstrips provide the position of the scattered electron and therefore the energy of the associated gamma-ray. Their pitch (300

μm) has been decided in order to limit the number of tagging channels without deterioration of the gamma-ray energy resolution imposed by the characteristics of the storage ring. The detector is in air, in a shielding box positioned inside a special section of the ring vacuum chamber. The shielding box is positioned at 10 mm from the circulating electron beam. This limits the lowest tagged gamma-ray energy to about 550 MeV.

3. Identification Events

The charged particle identification in the central part of apparatus (polar angles between 25 and 155 degree) was performed by using the bi-dimensional cut on the energy lost in the barrel versus the energy measured by the BGO calorimeter (see Fig.1 a)), while in the forward direction (for polar angle less than 25 degree) it was obtained by using the bi-dimensional cut on energy lost versus TOF measured by the plastic scintillator wall (see Fig. 1 b). We also applied to each detected charged particle the signal coincidence condition of three charged sensible detectors.

The information coming from direct measurements of the apparatus used in our data analysis are the energy E_γ of the incident photon measured by the tagging detector; the energy E_p of the proton measured in the BGO or by the TOF in the forward wall; the polar and azimuthal angles θ_p and ϕ_p of the proton and θ_{π^-} and ϕ_{π^-} of the pion measured by the planar and cylindrical MWPCs,[9,17] the energy of the pion E_{π^-} obtained by the reaction energy balance neglecting the Fermi energy of the neutron in the Deuterium target ($E_{\pi^-} = E_\gamma + M_n - E_p$). Our simulation, based on GEANT3[18] and on a realistic event generator[19] has shown that with the preliminary selection of the events obtained by the constrain of only one proton and only one charged pion in the Graal apparatus the number of events coming from concurrent channel is lower than 14%.

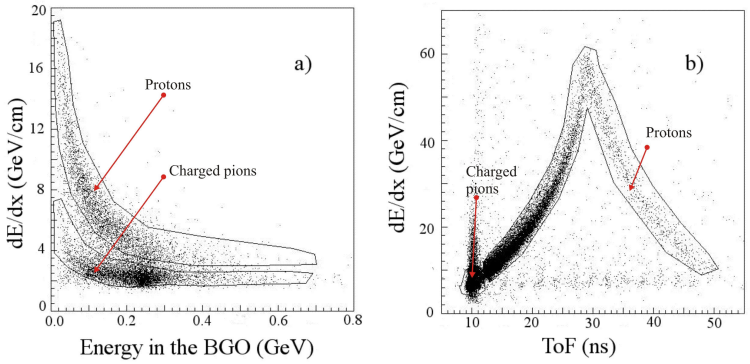

Fig. 1. Panel a): energy lost in the barrel vs. measured energy by the BGO; panel b): energy lost vs. TOF measured by the plastic scintillator wall.

4. Reconstruction of the Fermi Momentum

We reconstruct the Fermi momentum P_F (and consequently the Fermi energy E_F) by using the momentum conservation rules

$$\begin{aligned} P_{xF} &= P_{xp} + P_{x\pi^-} \\ P_{yF} &= P_{yp} + P_{y\pi^-} \\ P_{zF} &= P_{zp} + P_{z\pi^-} - E_\gamma \end{aligned} \tag{1}$$

We measure directly all quantities needed for the Fermi momentum reconstruction except the energy of the pion obtained by the energy balance neglecting the Fermi energy.

We try to improve the reconstruction of the Fermi momentum by a recursive procedure: we correct in the nth step calculation the estimation of the pion momentum by using the information of the Fermi energy calculated at the (n-1)th step. The iterations stop when the difference of the modules of the Fermi momentum in the two successive iterations is less than 10 keV/c. The cut value 10 MeV/c was suggest by the simulation in order to minimize the loss of good events (see Fig. 2)

In simulation, we observe that the difference between the Fermi momentum calculated at the nth and zero steps of the recursive method is small when we are considering signal events only(see solid line in Fig. 2). However, we find appreciable difference between these two values of Fermi momentum $P_F^n - P_F^0$ in the case of the concurrent channel (mainly the double charged pion photoproduction), then it is possible to use this quantity in order to distinguish the signal to the noise coming form the other channels (see dashed line in Fig. 2).

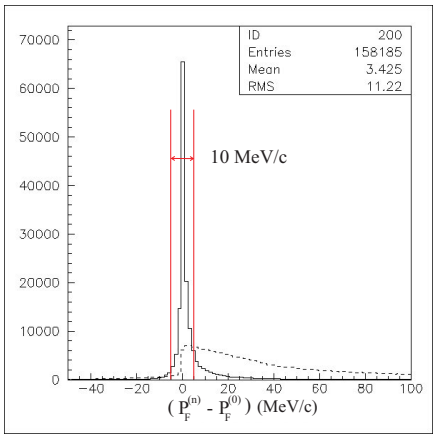

Fig. 2. In simulation, the difference between the Fermi momentum reconstruction at the nth step of recursive method and at zero-step for the signal (solid line) and for the concurrent channels (dashed line).

5. Single and Double Pion Photoproduction

The photoproduction of double charged pions can be considered a possible contamination source in the selection of events attributed to the $\gamma + p \rightarrow \pi^- + p$ reaction in the case that the apparatus miss the detection of one of two charged pion in the final state of reaction. In this section we consider the suppression of such a possible contamination by using the cut on the variable $P_F^n - P_F^0$ determined as described in the previous section.

By simple calculation it is easy to demonstrate that the Fermi momentum of participant in Deuterium for a three-body kinematic (double pion photoproduction) in the final state of reaction is given by the following formula

$$P_F = \sqrt{P^2_{F(\gamma+p\rightarrow\pi^-+p)} + P_m^2 + 2\sum_i^{x,y,z}(P_{im}P_{ip} + P_{im}P_{i\pi^-} - P_{im}E_\gamma)} \qquad (2)$$

where P_m is the momentum of the meson accompanying the couple π^- and proton.

Eq. 2 shows that the square of Fermi momentum calculated by a three-body kinematic is contributed by three terms: the first contribution coming from the two-body, the second is the square of momentum of the other meson, and the third is a sum of different component that make possible positive or negative contribution. In the cases that we apply the Eqs 1 for the reconstruction of the Fermi momentum, the procedure carries the mistake to attribute the amount of the missing momenta P_m and $(2\sum_i^{x,y,z}(P_{im}P_{ip} + P_{im}P_{i\pi^-} - P_{im}E_\gamma))$ to the P_{π^-}(the only quantity not measured directly) determining an overestimate Fermi momentum(see upper curve in Fig. 5, representing the overlap of the reconstruction cases of signal and concurrent channels). We find that this mistake amplifies the difference $P_F^n - P_F^0$ (see dashed line in Fig.2) and it justifies the possibility to use this variable difference as a further constraint in order to reduce the possible contamination coming from channels of double charged pions. In conclusion, we find that the more competitive channel was the $\gamma n \rightarrow \pi^-\pi^+ p$ process, and that the productions survive to all cuts only in the percentage of 0.2 in the following cases: i) the momentum of one pion

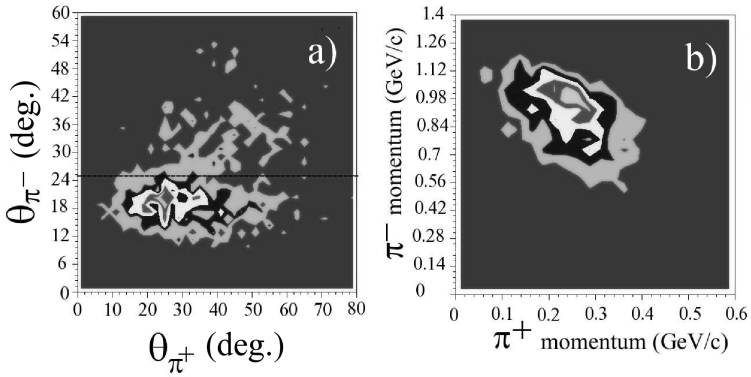

Fig. 3. In simulation, panel a) polar angle θ_{π^-} versus polar angle θ_{π^+}; panel b) momentum of π^- versus momentum of π^+ under condition $\theta_{\pi^-} < 25°$.

is very high in respect to the other one as showed in Fig. 3 a) (high difference in the direction of pions); ii) the difference between the polar angles of the pions are very little (see Fig. 3 b)).

6. Data Analysis

The measured quantities in the Graal-experiment provide an superabundant set of constraints. Then, it is possible to calculate all kinematic variables using only a subset of the measured ones. For example we are able to calculate the polar angle of the pion θ_{π^-} and the energy of the proton E_p^{calc} in the hypothesis of a pure two-body reaction.

We strongly reduced the background of the concurrent channels using different effective constraints:

- we combined the variables $x = \Delta\theta = \theta_{\pi^-}^{calc} - \theta_{\pi^-}^{meas}$ and $y = R_p = E_p^{calc}/E_p^{meas}$ in a bi-dimensional cut(see panel (a) of Fig. 4) selecting the events according to the condition

$$\frac{(x-\mu_x)^2}{\sigma_x^2} + \frac{(y-\mu_y)^2}{\sigma_y^2} - \frac{2C(x-\mu_x)(y-\mu_y)}{\sigma_x\sigma_y} < \sigma^2 \tag{3}$$

  where $\sigma = 3$, C is the correlation parameter obtained by a combined best fit of x and y with a bi-dimensional Gaussian surface, $\mu_{x\,or\,y}$ and $\sigma_{x\,or\,y}$ are the mean value and the variance obtained by a Gaussian fit to its experimental distribution. We find the parameters of the cuts by fitting the surface function (Fig. 4 a) for different energy of gamma and for different periods of data taking;[15,10]
- we impose the condition:

$$\sqrt{\sum_{i}^{x,y,z}(P_{Fi} - P_{Fi}^{recurs.})^2} < 10MeV/c \tag{4}$$

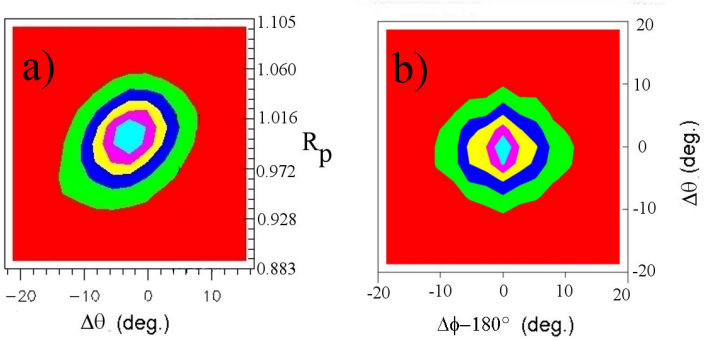

Fig. 4. In data, the bi-dimensional distribution $\Delta\theta$ vs. R_p (panel a) and $\Delta\theta$ vs. $|\phi_{\pi^-} - \phi_p - 180°|$ (panel b) as defined in the present paper.

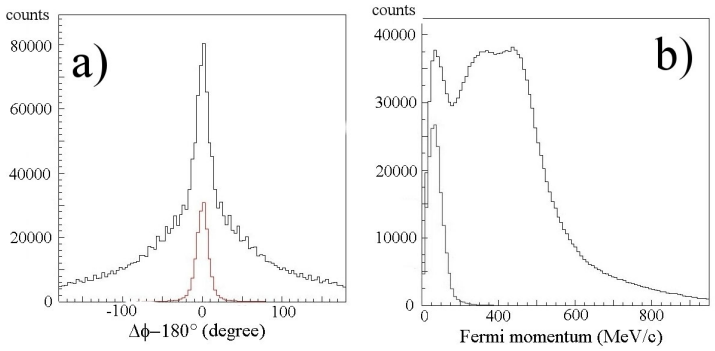

Fig. 5. In data, a) the π^--p coplanarity before (upper curve) and after the cuts (lower curve); b) the Fermi momentum of the neutron calculated before (upper curve) and after (lower curve) the cuts.

where: P_{Fi} (i=x,y,z) is the component of the Fermi momentum of the target nucleon calculated from the measured kinematic variables neglecting its Fermi energy; $P_{Fi}^{recurs.}$ is its value obtained at the end of a recursive process;

- we applied the condition on the coplanarity of the reaction products $(\Delta\phi - 180^\circ) < 3\sigma_{(\Delta\phi-180^\circ)}$ (see Fig. 5 a)), where $\Delta\phi = |\phi_p - \phi_{\pi^-}|$;
- we also reject all events where is present signal coming from neutral particle(the Graal detector can identify neutral particles see Refs.[9,10,15]).

We show the effect of the cuts on the degree of coplanarity of the reaction products (see Fig. 5 a) and on the Fermi momentum (see Fig. 5 b). By the simulation we estimate that after the described cuts the background of the concurrent reaction channel is lower than 2.3%.

To check the invariance of our results with respect to the selection criteria in a parallel analysis[a] we have:
i) plotted alternatively $\Delta\theta$ vs. $\Delta\phi$ which has the advantage of zero correlation as indicated in Fig. 4b;
ii) applied an independent cut on the variable R_p;
iii) introduced a cut for $P_F \leq 250$ MeV/c instead of the condition (1).

In Fig. 6 we present the comparison of the results of the two methods applied to independent periods of data acquisition using data of the vis-line of laser-beam (panel a) at low energy and data of the uv-line of laser-beam (panel b) at high energy. The results of the two procedures are mainly consistent within half sigma in many cases and within 1 sigma in some cases (see the two examples reported in Fig. 6).

We are able to reconstruct the reaction vertex by using the information coming from the MWPCs.[9,17] We verified that the reaction vertex of the selected events are correctly distributed inside the target region (see Fig. 7).

[a]francesco.mammoliti@ct.infn.it

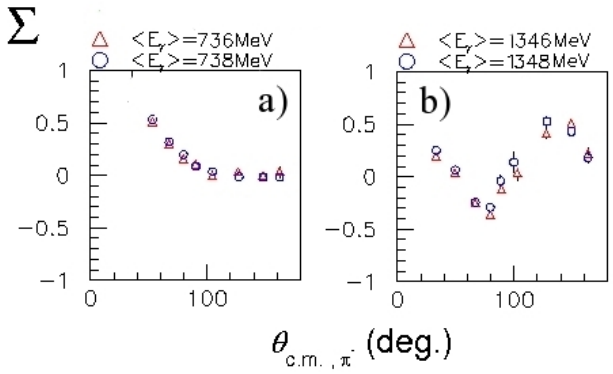

Fig. 6. Open circles, the beam asymmetry presented in this paper; open triangles, the results of the parallel analysis. Results obtained by independent data: vis-line(panel a) and uv-line (panel b).

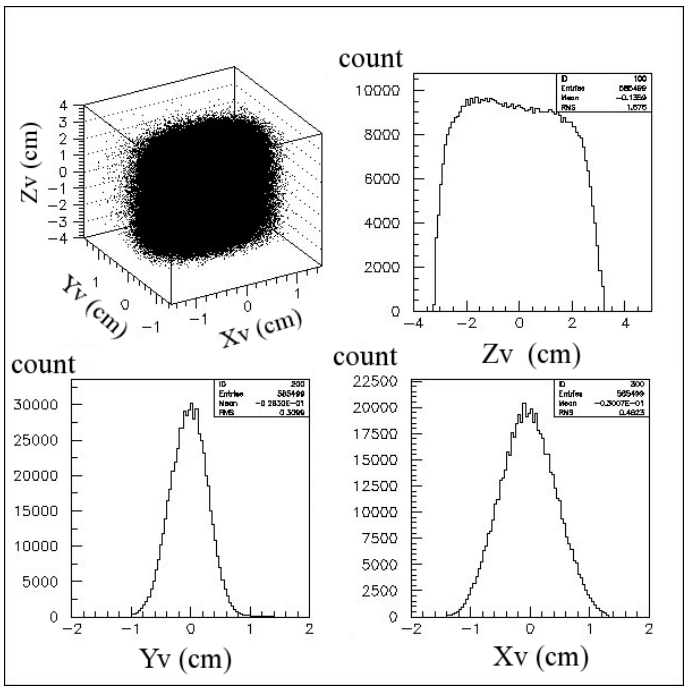

Fig. 7. Distribution of the reconstructed of reaction vertex in the Deuterium target.

The cuts realise a low Fermi momentum distribution; this is a suitable condition to have a quasi-free nucleon reaction. In the next section we present the preliminary data of the beam asymmetry extended also at backward angles and the first comparison with results of theoretical models;[20,21] we also include for a comparison the

previous experimental data[22] for smaller ranges of energy and angles. The beam polarization asymmetries have been calculated as indicated in Refs.[10,15] using the symmetry of the central detector around the beam axis. In the same references are indicated the various checks performed to verify the stability of our results.

7. Results and Conclusions

Our preliminary results of the asymmetries are reported in Fig.8 together with the previous data of Yerevan group[22] and some theoretical multipole analysis. SAID-GE09 is the solution that includes our results in the best fit while SAID-SP09 does not include them.[20] The MAID2007 solution is also included for a comparison.[21] The SAID-SP09 solution is consistent with our data in the forward angular region

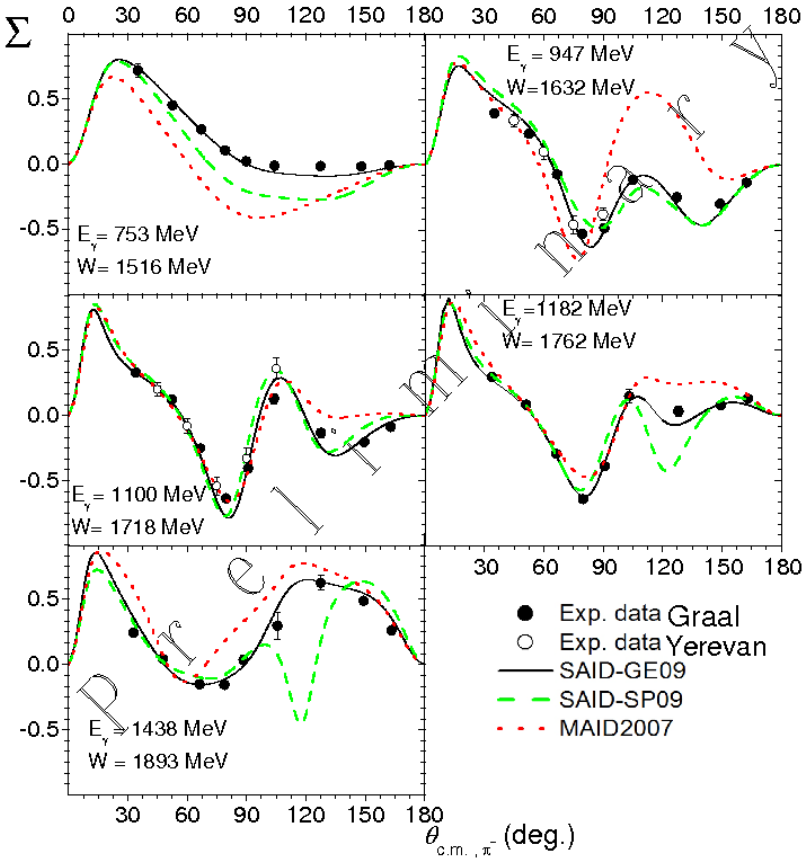

Fig. 8. Our preliminary beam asymmetries presented together with some previous results and theoretical curves. Full circles, our results; open circles, Yerevan results;[22] solid line, the SAID-GE09[20] calculation with inclusion of our data; dashed line, the SAID-SP09[20] calculation before the inclusion of our results; dotted line, the MAID2007[21] calculation.

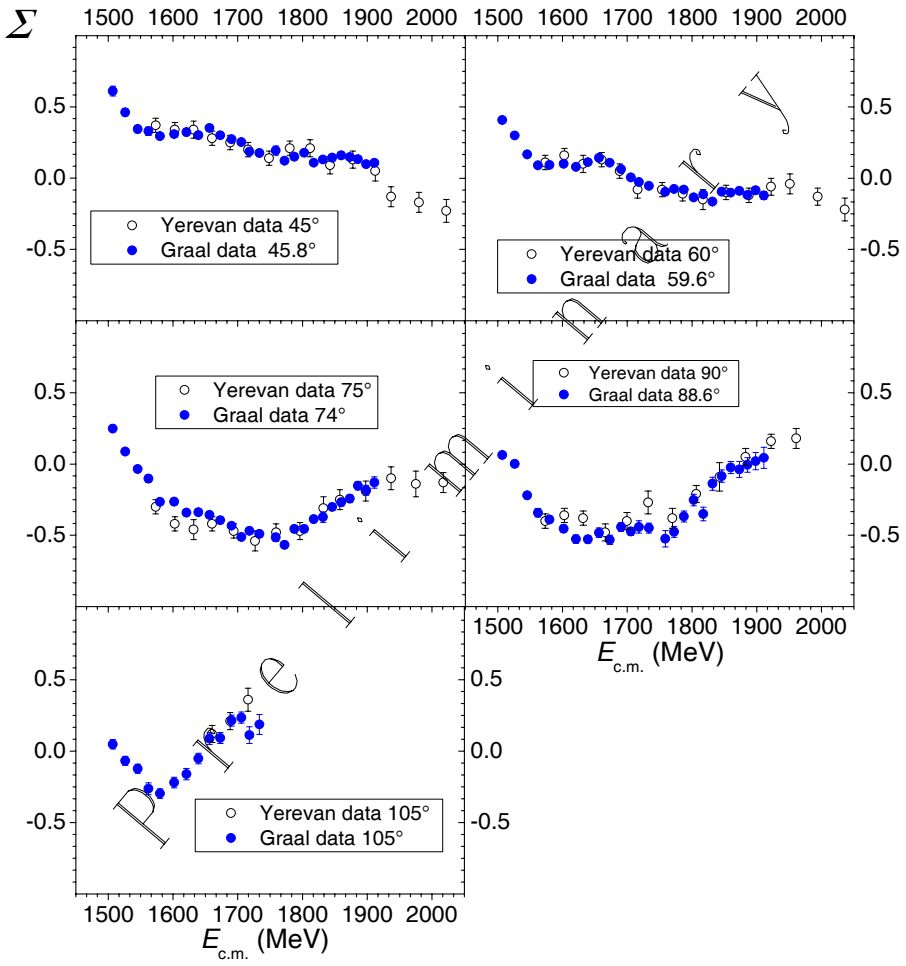

Fig. 9. Full circles our results, open circles the results of Ref.[22].

where the Yerevan results constrained the fit. In the backward angular region and at energies above 1100 MeV the agreement becomes satisfactory only after inclusion of our data. The MAID2007 solution agrees with our data in the forward region.

Our results are in substantial agreement with those of Yerevan[22] in the overlapping forward direction(see Figs. 8 and 9). The experiment[22] presented a very different detectors set up and gamma source in respect to the Graal-experiment, therefore the agreement between the two results represent a good test of the reliability of our analysis method and preliminary data. Our present results have considerably widened the energy and the angular range, and forced the theoretical model to improve the fit parameters.

Acknowledgments

We are grateful to the ESRF as a host institution for its hospitality and the accelerator group for the stable and reliable operation of the ring. The authors G. Mandaglio, M. Manganaro, and G. Giardina are grateful to G. Prestandrea and F. Cordaro of the CECUM of Messina, for their competent and active work in the maintenance of the workstation and data storage system of the group. We thank Igor Strakovsky for fruitful discussions and for his contribution in the fit of the asymmetry and the multipole analysis with the SAID model.

References

1. G.F. Chew, M.L. Goldberger, F.E. Low and Y. Nambu, *Phys. Rev.* **106** 1345 (1957).
2. M. Benmerrouche, N.C. Mukhopadhyay, J.F. Zhang, Phys. *Rev. D* **51** 3237 (1995).
3. B. Saghai, F. Tabakin, *Phys. Rev. C* **55** 917 (1997).
4. D. Drechsel, O. Hanstein, S.S. Kamalov, L. Tiator, *Nucl. Phys. A* **645** 145 (1999)
5. T. Feuster, U. Mosel, *Phys. Rev. C* **59** 460 (1999).
6. K.M. Watson, *Phys. Rev.* **95** 228 (1954).
7. R.L. Walker, *Phys. Rev.* **182** 1729 (1969).
8. O. Bartalini *et al.*, *Phys. Lett. B* **544** (2002) 113.
9. O. Bartalini *et al.*, *Eur. Phys. J. A* **A26** (2005) 399.
10. R. Di Salvo *et al*, *Eur. Phys. J. A* **42** (2009) 151.
11. L. Federici *et al*, *Il Nuovo Cimento B* **59** (1980) 247.
12. R. Caloi *et al*, *Lettere al Nuovo Cimento* **27** 339 (1980).
13. A. D'Angelo *et al*, *Eur. Phys. J. A* **31** (2007) 441 .
14. O. Bartalini *et al*, *Eur. Phys. J. A* **33** (2007) 169.
15. A. Fantini *et al*, *Phys. Rev. C* **78** (2008) 015203.
16. A. Lleres *et al*, *Eur. Phys. J A* **39** (2009) 149.
17. G. Mandaglio *et al*, *Radiat. Eff. Defects Solids* **164** (2009) 325.
18. *GEANT, Detector Description an Simulation Tool*, CERN program Library Long Writeup.
19. P. Corvisiero *et al*, *Nucl. Instr. & Meth. A* **346** (1994) 433.
20. http://gwdac.phys.gwu.edu/analysis/pr_analysis.html
21. http://www.kph.uni-mainz.de/MAID//maid2007/polariz.html
22. F.V. Adamian, P.I. Galumian, V.H. Grabsky, H.H. Hakopian, V.K. Hoktanian, G.V. Karapetian, V.V. Karapetian and H.H. Vartapetian, *J. Phys. G: Nucl. Part. Phys.* **15** 1797 (1989).